A homozygous PIWIL2 frameshift variant affects the formation and maintenance of human induced pluripotent stem cell-derived spermatogonial stem cells and causes Sertoli cell only-syndrome

Xiaotong Wang
Huazhong University of Science and Technology Tongji Medical College
Zili Li
Huazhong University of Science and Technology Tongji Medical College
Mengyuan Qu
Huazhong University of Science and Technology Tongji Medical College
Chengliang Xiong
Huazhong University of Science and Technology Tongji Medical College
Honggang Li (lhgyx@hotmail.com)
Huazhong University of Science and Technology https://orcid.org/0000-0002-6666-8527

Research Article

Keywords: male infertility, Sertoli cell-only syndrome, PIWIL2, induced pluripotent stem cell, spermatogonial stem cell

Posted Date: July 14th, 2022

DOI: https://doi.org/10.21203/rs.3.rs-1773547/v1

Abstract

Background

The most serious condition of male infertility is complete Sertoli cell-only syndrome (SCOS), referring to lack of all spermatogenic cells in testes. Genetic cause of SCOS remains to be explored. We aimed to investigate the genetic cause of SCOS and assess the effects of the identified causative variant on human male germ cells.

Methods

Whole-exome sequencing was performed to identify potentially pathogenic variants in a man with complete SCOS and Sanger sequencing was performed to verify the causative variant in this man and his father and brother. The pathogenic mechanisms of the causative variant were investigated by *in vitro* differentiation of human induced pluripotent stem cells (hiPSCs) into germ cell-like cells.

Results

The homozygous loss-of function (LoF) variant p.His244ArgfsTer31 (c.731_732delAT) in *PIWIL2* was identified as the causative variant in the man with complete SCOS, and the same variant in heterozygosis was confirmed in his father and brother. This variant resulted in a truncated PIWIL2 protein lacking of all functional domains, and no PIWIL2 expression was detected in the patient's testes. The patient and $PIWIL2^{-/-}$ hiPSCs could be differentiated into primordial germ cell-like cells and spermatogonial stem cell-like cells (SSCLCs) *in vitro*, but the formation and maintenance of SSCLCs were severely impaired. RNA-seq analyses proposed inactivation of the Wnt signaling pathway in the process of SSCLC induction in the $PIWIL2^{-/-}$ group, which was validated in the patient group by RT-qPCR. The Wnt signaling pathway inhibitor hindered the formation and maintenance of SSCLCs during the differentiation of normal hiPSCs.

Conclusions

Our study revealed the pivotal role of PIWIL2 in the formation and maintenance of human spermatogonial stem cells. We provided clinical and functional evidence that the LoF variant in *PIWIL2* is a genetic cause of SCOS, which supported the potential role of *PIWIL2* in genetic diagnosis. Furthermore, our results highlighted the applicability of *in vitro* differentiation models to function validation experiments.

Background

Male infertility affects approximately 7% of the male population [1], and azoospermia cases represent 10–20% of male infertility cases [2]. Non-obstructive azoospermia (NOA) is a spectrum of spermatogenic quantitative defects, which accounts for the majority of azoospermia (> 70%) and affects 1% of adult male population [2, 3]. NOA includes three patterns of testicular histology, hypospermatogenesis, maturation arrest, and Sertoli cell-only syndrome (SCOS). SCOS, affecting 26.3–57.8% of men with azoospermia [4], is characterized by a lack of spermatogenic cells but only Sertoli cells remaining in seminiferous tubules. Complete SCOS is the most serious condition wherein all observed seminiferous tubules of testicular biopsy only contain Sertoli cells, whereas incomplete SCOS means spermatogenic areas remain in testes. Men with azoospermia have the highest risk of being affected by genetic anomalies [1]. The etiology of SCOS involves genetic factors. Already known genetic causes have been applied in the clinical etiologic diagnosis of SCOS are karyotype abnormalities and microdeletions of azoospermic factor on the Y chromosome. Unfortunately, a large proportion of SCOS cases remain unexplained [5] and the etiology and pathogenesis of SCOS have not been fully elucidated to date.

To gain insight into etiology and pathogenesis of SCOS, we referred to mouse models with Sertoli cell-only (SCO) phenotype; for instance, *Prdm14*$^{-/-}$, *Tcfap2c* $^{flox/flox}$:*Sox2-cre*, *Fancb*$^{-/-}$, *Id4*$^{-/-}$, *Zfp145*$^{-/-}$, and *Wt1*$^{-/flox}$; *Cre-ER™* mice have the testicular phenotype similar to human SCOS [6–11]. According to these mouse models, abnormalities in primordial germ cells (PGCs), spermatogonial stem cells (SSCs) or Sertoli cells can lead to the absence of spermatogenic cells after birth, resulting in SCO phenotype. In recent years, whole exome sequencing (WES) has been performed in men with SCOS from consanguineous and non-consanguineous families, revealing several pathogenic or potentially pathogenic variants in genes, such as *FANCA*, *FANCM*, *TEX15*, *KLHL10*, *DMRT1*, *USP26*, *NANOS2*, *TEX14*, and *WNK3* [3, 12–15]. Among these genes, *FANCM*, *DMRT1*, and *NANOS2* have corresponding gene knockout mouse models that exhibit a phenotype similar to human SCOS [14, 16, 17]. As at least 2,000 genes are involved in spermatogenesis [1] and various mouse models manifest SCO phenotype, new genes implicated in human SCOS are expected to be identified. On the other hand, germ cell development is an important issue for fertility and inheritance. Identifying genes that can lead to SCOS could be an approach to identify candidate genes involved in human germ cell development.

Because the mouse and human reproductive systems are not identical and genes may have different functions or transmit disease through different modes of inheritance, caution is urged to draw conclusions on gene function and inheritance mode based on mouse models only [18]. Differentiation of human induced pluripotent stem cells (hiPSCs) into human male germ cell-like cells could provide a better *in vitro* disease model to study male infertility [19]. This approach bypasses the ethical and technical problems on using human primary germ cells for functional experiments, also generates large numbers of primordial germ cell-like cells (PGCLCs) and spermatogonial stem cell-like cells (SSCLCs) in a short time [20–24]. Furthermore, this approach could be a *in vitro* model to study genotype-phenotype correlations because hiPSCs and differentiated cells retain patient's genetic background.

In this study, we applied WES in a man with complete SCOS and identified a homozygous frameshift deletion variant in *PIWIL2* as the genetic cause of SCOS. *PIWIL2* is the ortholog of murine *Mili* and

encodes a protein that represses the activity of transposons via piRNA pathway. Mutations of other PIWI family members in male infertility have attracted much attention [25, 26]. Recent studies also suggested *PIWIL2* as the candidate gene of male infertility in men [27], although without functional validation. Deletion of *Mili* in mouse causes meiosis arrest or incomplete SCO phenotype [28, 29], which is not identical to the complete SCOS testicular histology of the patient included in our study. Furthermore, the expression of PIWIL2 in germ cells is different between mice and humans [30]. We suspected that PIWIL2 might have different roles in regulating human germ cell development and spermatogenesis. Using *in vitro* differentiation models, we found evidence that the identified variant in *PIWIL2* affected the formation and maintenance of SSCLCs, along with dysregulation of the Wnt signaling pathway. These results supported that the LoF variant in *PIWIL2* leads to human SCOS.

Methods

Participants

We retrospectively reviewed all patients with NOA who visited our institute from 13, January 2014 to 8, October 2015 to choose patients with complete SCOS according to the following criteria: i) testicular biopsy showed completely loss of spermatogenic cells in all observed seminiferous tubules, and ii) seminal *DDX4* mRNA negative [5]. Patients with known genetic causes, including abnormal karyotype or AZF microdeletions, and with no results of karyotype or AZF microdeletions tests were excluded. The patient included in the present study was one of the patients with complete SCOS who agreed to be enrolled to provide with gnomic DNA (gDNA) for WES. He (Figure 1A, IV1) came from a consanguineous family in which his parents were first-cousins. He had no general health problems. The clinical parameters were listed in Table 1. He and his wife had a child through intrauterine artificial insemination by donor, suggesting that his wife was fertile. His relatives claimed that they did not suffer from infertility. His younger brother had normal semen analysis results. His sister has two daughters. His father (Figure 1A, III1) and younger brother (Figure 1A, IV2) agreed to participate in our study to provide with gDNA. His mother had been disconnected from his family for years, and thus was not included in this study.

All the people included in this study had signed informed consent.

Whole exome sequencing and data analysis

Total gDNA was isolated from peripheral blood using QIAamp DNA Blood Mini Kit (Qiagen, Germany) and passed integrity assess. After fragmented with Covaris-focused ultrasonication, DNA was used to prepare sequencing library using SureSelect Human All Exon v6 Kit (Agilent, USA). Sequencing was performed on an Illumina HiSeq 2500 platform. We got 14.2 G clean data. The percentage of base above Q30 was 88.1%. The mean sequencing average depth was 123.8 and 20X sequence coverage was 94.3%. Sequencing reads were aligned to human genome (GRCh37/hg19) using Burrows-Wheeler Aligner before removing adaptors, PCR duplicates and low-quality reads. Single nucleotide substitutions and indel variants were called with Genome Analysis Toolkit (GATK) (12). The detected variants were annotated with Ensembl and variants with genomic frequency MAF $\geq$ 0.01 in ExAC, gnomAD, or 1000 Genomes

Project were excluded. Considering that the patient was from a consanguineous family, homozygous and hemizygous variants were retained for further screening. Variants affected protein sequence and missense variants that were predicted to be deleterious by at least half of the software (SIFT, PolyPhen 2 HDIV, PolyPhen 2 HVAR, and Mutation Taster) were further kept. We next screened and kept genes that are expressed in human testis and function during spermatogenesis.

PCR and Sanger sequencing

gDNA was extracted from human peripheral blood or hiPSCs, and used to amplify *PIWIL2* fragment with TAKARA Ex Taq (TAKARA, Japan) on a SimpliAmp Thermal Cycler (Thermo Fisher Scientific, USA). The specific primers were listed in Additional File Table 1. PCR products were sequenced on a 3730XL DNA Analyzer with forward primers, and the results were viewed on the Chromas.

Histological analysis and immunohistochemistry

Testicular samples derived from testicular biopsy were fixed with 4% paraformaldehyde and embedded with paraffin. For histological analysis, testicular sections were prepared and stained with hematoxylin and eosin. For the detection of PIWIL2 protein, testicular sections were prepared and blocked with 5% bovine serum albumin (BSA), followed by incubation with PIWIL2 or isotype (all from Abcam, UK) primary antibody (Additional File Table 2) at 4 °C overnight. After incubated with secondary antibody (Additional File Table 2) at room temperature for 1 hour, sections were visualized with the use of DAB Horseradish Peroxidase Color Development Kit (Beyotime, China). Nuclei were stained with hematoxylin. The sections were then observed under an Olympus microscope.

Cell culture

The hiPSC line of the patient was generated from fibroblasts derived from the skin specimen of testicular biopsy incision. The normal hiPSC line was generated from fibroblasts derived from foreskin of a fertile volunteer. These two hiPSC lines have been described elsewhere [31,32]. The homozygous c.731_732delAT variant in *PIWIL2* in hiPSCs of the patient was confirmed using Sanger sequencing, and the normal hiPSCs were wild-type at the same location [22]. The hiPSCs were seeded on Matrigel (Corning, USA)-covered plates and maintained in mTeSR 1 medium (STEMCELL Technologies, Canada) at 37 °C, 5% CO_2, and the medium was changed every day. hiPSCs were passaged every 3-4 days at a ratio of 1:3 using 0.5 mM EDTA.

Knockout of *PIWIL2* in normal hiPSCs

Single guide RNA (AGACCTCCGTTGGTTGGAGTAGG) plasmids (pX330) targeting exon 4 of *PIWIL2* were constructed. Plasmids (1 μg) were transfected into hiPSCs (2×10^5/ per well of 6-well plate) by 3 μL Lipofectamine Stem Transfection Reagent (Thermo Fisher Scientific, USA). Cells were allowed to grow into colonies from single cells and the colonies were manually picked for Sanger sequencing to recognize

the homozygous and heterozygous mutant colonies. *PIWIL2*$^{-/-}$ and PIWIL2$^{+/-}$ colonies were retained for further studies.

Western blot

Proteins from testicular tissues and cells were extracted using RIPA buffer containing PMSF. After centrifuged at 12,000 × *g* for 15 minutes at 4 °C, the supernatant containing proteins was mixed with loading buffer and denatured. Proteins were separated on 10% SDS-PAGE gel and transferred to PVDF membranes (Millipore, USA). The membranes were blocked with 5% BSA and incubated with PIWIL2 (Abcam, UK) and β-Actin (Proteintech, Chima) primary antibodies (Additional File Table 2) at 4 °C overnight. The membranes were then incubated with secondary antibodies (Additional File Table 2) at room temperature for 1 hour and visualized using a BeyoECL Plus kit (Beyotime, China) on a ChemiDoc XRS+ System (Bio-Rad, USA).

Cell counting kit-8 assay

The cell proliferation rate was measured using the Cell Counting Kit-8 (Beyotime, China) according to the manufacturer's protocol.

In vitro differentiation of hiPSCs into germ cell-like cells

In vitro differentiation of hiPSCs into PGCLCs and SSCLCs was performed as previously described [21,22].

Flow cytometry

PGCLCs were dissociated and stained with ITGA6 (BD, USA) and EpCAM (BD Biosciences, USA) primary antibodies (Additional File Table 2) [21]. SSCLCs were dissociated with Accutase (Thermo Fisher Scientific, USA) and stained with PLZF (Invitrogen, USA) primary antibody (Additional File Table 2) after fixing, permeabilizing and blocking processes [22]. The percentages of PGCLCs and SSCLCs were determined by a flow cytometer (Beckman Coulter, USA).

RT-qPCR

Total RNA was extracted from cells using TRIzol (Thermo Fisher Scientific, USA) and then reverse-transcribed into cDNA using HiScript III RT SuperMix (Vazyme, China) on a SimpliAmp Thermal Cycler (Thermo Fisher Scientific, USA). RT-qPCR was conducted with ChamQ Universal SYBR qPCR Master Mix (Vazyme, China) on a StepOne Real-Time PCR system (Thermo Fisher Scientific, USA). Primers used in this study were listed in Additional File Table 1. *β-Actin* was used as the internal control. Gene expression was assessed using $2^{-\Delta\Delta CT}$ method.

Immunofluorescence

Cells were fixed with 4% paraformaldehyde for 15 minutes at room temperature. After washed with PBS, cells were blocked and permeabilized with 5% BSA containing 0.3% Triton X-100 for 45 minutes at room temperature. Cells were then incubated with PLZF (Santa Cruz, USA) and GPR125 (GeneTex, USA) primary antibodies (Additional File Table 2) at 4℃ overnight, followed by incubated with secondary antibodies (Additional File Table 2) at room temperature for 1 hour. Nuclei were stained with DAPI. Cells were observed under a fluorescence microscope (Olympus, Japan).

RNA-seq and data analysis

Total RNA was extracted from biological duplicates of cells from each group and used to construct RNA-seq libraries using a TruSeq Stranded mRNA Kit (Illumina, USA). Libraries were sequenced using the Illumina NovaSeq 6000 platform. After removing the adaptor sequence and low-quality reads, clean reads were mapped to the human genome GRCh38/hg38 using HISAT2. The aligned reads of genes were counted and normalized to evaluate gene expression as normalized counts per million by Stringtie. Significantly differentially expressed genes were those with false discovery rate (FDR) <0.05 and $|\log_2(\text{fold change})| > 1$ assessed by edgeR. Pathway analyses were performed using KOBAS 3.0 (http://bioinfo.org/kobas) [33].

Statistical analysis

Data are presented as mean ± SD. Statistical analyses were conducted with One-way ANOVA using GraphPad Prism 9, and figures were also created with this software. $P < 0.05$ was considered statistically significant.

Results

Clinical characterization of the man with complete SCOS

The clinical parameters of the patient (Figure 1A, IV1) were summarized in Table 1. He has a normal karyotype (46, XY) and no microdeletions on the Y chromosome. The testicular volume on both sides was reduced, but serum hormone levels (total /free testosterone, follicle stimulating hormone, and luteinizing hormone) were normal. Semen analyses indicated no sperm was present. Additionally, increased seminal elastase level implied genital tract infection. Testicular histology showed that all the observed seminiferous tubules did not contain spermatogenic cells, representing complete SCOS (Figure 1D). The absence of seminal *DDX4* (a germ cell specific gene) mRNA can serve to discriminate complete SCOS more accurately [5]. The seminal *DDX4* mRNA test result of the patient was negative, which confirmed the testicular histology of complete SCOS.

Identification of potential pathogenic variants from WES data

We performed WES analysis of the patient to screen potentially pathogenic variants responsible for infertility. Considering the consanguineous background and the fact that the patient was the only infertile

case in his family, we retained likely causative variants by filtering the WES data according to (i) genomic frequency MAF < 0.01, (ii) the recessive inheritance mode, and (iii) functional impact on protein sequence and predicted to be deleterious. Finally, eight potential disease-causing variants in eight genes (Additional File Table 3) were identified for the manual screening of their expression in testis and roles in spermatogenesis. A frameshift deletion variant p.His244ArgfsTer31 (c.731_732delAT) mapped to *PIWIL2* gene caught our attention because *PIWIL2* is the only gene that is expressed in testis and associated with male infertility in mice among these eight genes [28,29]. Spermatogenesis of *Mili*$^{-/-}$ mice was blocked at the early prophase of the first meiosis, resulting in an incomplete SCO phenotype that most seminiferous tubules were depleted of spermatogonia [28,29]. A homozygous missense variant (c.745C>T) and a homozygous non-frameshift deletion variant (c.727_729del) in *PIWIL2* in two patients with NOA have been reported [27], but the effects of these two variants on protein function were not as serious as the variant identified in our study. Therefore, the homozygous frameshift deletion variant in *PIWIL2* was suspected to be the causative variant of infertility in this patient. Sanger sequencing confirmed c.731_732delAT in *PIWIL2* in the patient, and his father and brother carried the same variant in heterozygosis (Figure 1B), implying that his mother also carried the same heterozygous variant in *PIWIL2* and the inheritance mode of this variant was indeed autosomal recessive.

PIWIL2 is located on human chromosome 8 and encodes a protein belonging to PIWI family. The PIWIL2 protein consists of 973 amino acids (aa) and contains three domains, Argonaute linker 1 domain (339..386 aa), PAZ domain (387..504 aa), and PIWI domain (512..956 aa). The conserved functions of PAZ domain and PIWI domain are RNA binding and RNA silencing [34,35], respectively. In this study, the identified variant in *PIWIL2* was a two-nucleotide deletion in exon 6, which introduced a premature stop codon and was predicted to result in a truncated protein of 273 aa that lacked all functional domains (Figure 1C). We used a PIWIL2 antibody whose immunogen was in middle part of the PIWIL2 protein (410..460 aa) to label PIWIL2 protein expressed in patient's testes and human testes with normal spermatogenesis. No positive signal was observed in seminiferous tubules of the patient's testicular tissues, but PIWIL2 was shown to be expressed in spermatogonium, spermatocytes and round spermatids in testes with normal spermatogenesis (Figure 1E). Hence, the homozygous frameshift deletion variant in *PIWIL2* resulted in a truncated PIWIL2 protein that could not exert effects on human germ cells.

The LoF variant in *PIWIL2* did not affect PGCLC specification

To validate the effects of the LoF variant in *PIWIL2* on human germ cells and explore the role of PIWIL2 in human germ cell development, we employed *in vitro* differentiation of hiPSCs into germ cell-like cells models. This approach circumvents the difficulties and ethical issues in obtaining human primary germ cells for functional experiments. The hiPSC line of the patient shares the same genetic background as its donor cell; it retained the homozygous c.731_732delAT variant in *PIWIL2* as in the patient with SCOS [32]. We also used CRISPR/Cas9 to introduce a homozygous frameshift deletion in *PIWIL2* (*PIWIL2*$^{-/-}$) in the normal hiPSC line (control), leading to a truncated PIWIL2 protein (165 aa) nearly equivalent to the truncated PIWIL2 protein expressed in testes of the patient (Additional File Figure 1A and B). The

PIWIL2$^{+/-}$ hiPSC line was also retained to simulate the variant carried by the patient's father and brother (Additional File Figure 1B). The expression of PIWIL2 was confirmed in hiPSC lines using western blot (Figure 2A). The expression of pluripotent genes and cell proliferation in *PIWIL2*$^{-/-}$ and *PIWIL2*$^{+/-}$ hiPSC lines were comparable to that in normal hiPSC line (Additional File Figure 1C).

PIWIL2 is firstly expressed in late PGCs [30]. We explored whether the LoF variant in *PIWIL2* affected human PGCs using a known *in vitro* differentiation model of differentiating hiPSCs into PGCLCs [31]. At 4 days of differentiation when PGCLCs were abundant, the percentage of PGCLCs was decreased in the *PIWIL2*$^{-/-}$, *PIWIL2*$^{+/-}$,and patient groups compared with the control group ($p < 0.05$), but the difference was not significant in the *PIWIL2*$^{-/-}$ group compared with the *PIWIL2*$^{+/-}$ group (Figure 2B, Additional File Figure 1D). Thus, the LoF variant in *PIWIL2* and deletion of PIWIL2 did not affect the specification of human PGCs.

The LoF variant in *PIWIL2* affected SSCLC formation and maintenance

We further differentiated hiPSCs into SSCLCs to investigate whether the LoF variant in *PIWIL2* could cause abnormalities in human SSCs. The SSCLC induction efficiency was reduced in the *PIWIL2*$^{-/-}$ and patient groups at 8, 10, 12 and 14 days of differentiation when compared with the control group, and the induction efficiency in the *PIWIL2*$^{-/-}$ group was also lower than that in the *PIWIL2*$^{+/-}$ group ($p < 0.05$) (Figure 2C, Additional File Figure 2). RT-qPCR was performed to determine the expression of SSC-related genes after 12 days of differentiation. Similar to the trends of SSCLC induction efficiency, the expression of SSC-related genes, including *PLZF*, *ID4*, *GFRα1*, *TSPAN33*, *LPPR3*, and *NANOS2* was significantly lower in the patient and *PIWIL2*$^{-/-}$ groups when compared with the control group, and the gene expression in the *PIWIL2*$^{-/-}$ group was also significantly lower than that in the *PIWIL2*$^{+/-}$ group (Figure 2D). Immunofluorescence results showed that the staining of co-expressed PLZF and GPR125 that represented SSCLCs was weak and less intensive in the patient and *PIWIL2*$^{-/-}$ groups than that in the control and *PIWIL2*$^{+/-}$ groups after 12 days of differentiation (Figure 2E). Moreover, from 12 to 14 days of differentiation, the induction efficiency in the control and *PIWIL2*$^{+/-}$ groups remained at a stable level, whereas the induction efficiency in the patient and *PIWIL2*$^{-/-}$ groups declined (Figure 2C). These results suggested that the LoF variant in *PIWIL2* and deletion of PIWIL2 affected the formation and maintenance of SSCLCs.

Transcriptome analyses of hiPSCs and cells at 8 and 12 days of SSCLC induction

Next, we analyzed the transcriptome of hiPSCs (day 0 of differentiation) and cells at 8 and 12 days of SSCLC induction from the control and *PIWIL2*$^{-/-}$ groups. In hiPSCs, only 136 differentially expressed genes (DEGs) were found between the control and *PIWIL2*$^{-/-}$ groups (Additional File Figure 3A, Additional File Table 4). At 8 days of differentiation, when SSCLCs emerged, 6125 and 4472 DEGs were found in the control (3475 upregulated and 2650 downregulated) and *PIWIL2*$^{-/-}$ (2791 upregulated and 1681 downregulated) groups, respectively, compared with corresponding hiPSCs (Additional File Figure 3B). At

12 days of differentiation, more DEGs were identified. There were 4489 upregulated genes and 3213 downregulated genes in the control group, and 3831 upregulated genes and 2186 downregulated genes in the *PIWIL2*$^{-/-}$ group, compared with the corresponding hiPSCs (Additional File Figure 3C). SSCLC induction process induced a global change in transcriptome, but deletion of PIWIL2 seemed to affect gene expression profile.

We compared the transcriptome of control and *PIWIL2*$^{-/-}$ groups at 8 and 12 days of SSCLC induction. At 8 days of differentiation, there were 1200 upregulated genes and 786 downregulated genes between these two groups (Figure 3A). At 12 days of differentiation, the number of upregulated genes were 1114, but the number of downregulated genes increased to 981 (Figure 3A). KEGG analyses revealed that DEGs were involved in TGF-beta signaling pathway, MAPK signaling pathway, Hippo signaling pathway, and Wnt signaling pathway (Figure 3B, Additional File Figure 3D). We noticed that the downregulated genes in the control and *PIWIL2*$^{-/-}$ groups were both enriched in “Wnt signaling pathway” and “Signaling pathways regulating pluripotency of stem cells” at 8 and 12 days of differentiation (Figure 3B). Wnt signaling pathway genes were downregulated but pluripotent genes were upregulated in the *PIWIL2*$^{-/-}$ group compared to those in the control group (Figure 3C). Additionally, SSC-related genes were downregulated in the *PIWIL2*$^{-/-}$ group, but the expression of genes related to endoderm and mesoderm was not obviously altered (Figure 3C). Transcriptome analysis indicated that deletion of PIWIL2 failed to induce the expression of Wnt signaling pathway genes and SSC genes and repress pluripotent genes during differentiation, but the development of germ layers was not affected. We confirmed the expression of genes in Wnt signaling pathway and pluripotency in the control and *PIWIL2*$^{-/-}$ groups at 8 and 12 days of differentiation by RT-qPCR, and the results showed the same trends as the transcriptome analysis (Figure 3D). Decreased expression of genes in Wnt signaling pathway and increased expression of pluripotent genes were also confirmed in the patient group, and the trends of gene expression in the *PIWIL2*$^{+/-}$ group were similar to those in the control group (Figure 3D).

Inactivated Wnt signaling pathway might affect SSCLC formation and maintenance

We suspected that impaired formation and maintenance of SSCLCs might be associated with the inactivated Wnt signaling pathway. We added IWR-endo-1 (a Wnt signaling pathway inhibitor) to the SSCLC induction medium of the control group from day 1, 10, and 12 of differentiation and detected the SSCLC induction efficiency and the expression of *PLZF* on 12 or 14 days of differentiation. When IWR-endo-1 was added to the medium from day 1, the SSCLC induction efficiency was significantly decreased compared to normal differentiation at day 12 ($p < 0.05$) (Figure 4A). Two days of treatment with IWR-endo-1 from day 10 to day 12 also reduced the SSCLC induction efficiency detected on day 12 ($p < 0.05$) (Figure 4A). Moreover, treatment with IWR-endo-1 from day 12 reduced the percentage of SSCLCs detected on day 14 ($p < 0.05$) (Figure 4B). These results indicated that inhibition of Wnt signaling pathway impaired the formation and maintenance of SSCLCs. Deletion of PIWIL2 might inactivate Wnt signaling pathway thus abolishing the formation and maintenance of SSCLCs.

Discussion

In this study, we performed WES on a man with complete SCOS and identified the LoF variant p.His244ArgfsTer31 (c.731_732delAT) in *PIWIL2*. We further revealed that the LoF variant in *PIWIL2* could impair the formation and maintenance of human SSCLCs, which was associated with inactivation of Wnt signaling pathway. Clinical and functional evidence suggested that *PIWIL2* is a causative gene of SCOS. Our study reinforced the understanding that the etiology of NOA involves multiple genes, and we provided a new gene for SCOS.

To date, the association between *PIWIL2* and infertility in humans has not yet been fully explained. A homozygous missense variant (c.745C > T) and a homozygous non-frameshift deletion variant (c.727_729del) in *PIWIL2* were found in two independent patients with NOA, but these two variants have not been validated by functional experiments or in a larger group of infertile men [27]. Other studies showed that SNPs in *PIWIL2* (rs4871990 and rs13259097 in the promoter) were not associated with the risk of azoospermia and oligozoospermia, but SNPs in the other two members of PIWI family, *PIWIL4* (rs508485) and *PIWIL3* (rs11703684), were significantly associated with the risk of oligozoospermia [36–38]. Our study reported a homozygous frameshift deletion variant in *PIWIL2* in a man with complete SCOS, and this variant greatly affected the function of PIWIL2. The patient's father and brother were heterozygous carriers, suggesting that the heterozygous frameshift variant in *PIWIL2* may not affect male infertility.

The current knowledge of PIWIL2 in spermatogenesis originates mainly from mouse models. PIWIL2 (MILI) is the earliest PIWI protein expressed in male germ cells from late PGC stage to round spermatid stage in mice [39]. MILI mainly performs the homotypic ping-pong cycle to silence transposons in a piRNA-dependent manner and produce piRNAs that associate with MIWI2 [39]. SSCs of *Mili*$^{-/-}$ mice could not complete self-renewal and differentiation; hence, spermatogenesis was blocked at the early prophase of the first meiosis, and most seminiferous tubules were depleted of spermatogonia by 180 days postpartum, resulting in an incomplete SCO phenotype [28, 29]. The SCO phenotype of *Mili*$^{-/-}$ mice was similar to that of the patient included in our study, suggesting that the LoF variant in *PIWIL2* affected male infertility and caused SCOS phenotype. However, the testicular phenotype of the patients was complete SCOS, other than the incomplete SCO in *the Mili*$^{-/-}$ mice. This difference implies that the impairment in human SSCs of the patient may occur earlier than that in mice.

Meiotic arrest in mice caused by knockout of *Mili* was suggested to be associated with desuppression of transposons through piRNA pathway [40]. In humans, PIWIL2 is expressed in cytoplasm of PDPN^{+}/DDX4^{-} germ cells (late PGC stage) and in cytoplasm and nuclei of some PDPN^{-}/DDX4^{+} germ cells (fetal spermatogonia stage), spermatogonium and spermatocytes, and strongly accumulates in nuclei of spermatids [30]. In mice, MILI is expressed in cytoplasm of male germ cells [30]. Moreover, PIWIL4, but not PIWIL2, is present in intermitochondrial cement of human PDPN^{-}/DDX4^{+} germ cells [30]. In contrast, in mice, MILI exists in intermitochondrial cement, whereas MIWI2 is in piP-bodies [30]. The different expression patterns and locations of PIWIL2 between humans and mice suggested that the

exact role of PIWIL2 in germ cell development and spermatogenesis might be different between these two species.

To determine whether the LoF variant in *PIWIL2* is indeed the cause of SCOS, we used *in vitro* differentiation models to generate human germ cell-like cells. *In vitro* models circumstance the problem that human germ cells are difficult to obtain, purify, and culture, and target deletion or over-expression of genes can be easily performed in this system [41]. *In vitro* differentiation models could be a new approach to directly study human germ cells and identify unique mechanisms in human reproduction [41]. Our findings demonstrated that the LoF variant in *PIWIL2* and the homozygous deletion of *PIWIL2* did not affect the specification of PGCLCs but impaired the formation and maintenance of SSCLCs. These findings provided direct evidence that the LoF variant in *PIWIL2* affected the formation and maintenance of human SSCs and thus caused SCOS. Interestingly, deletion of MILI in mice did not affect the formation of SSC population but hindered the SSC self-renewal and differentiation into pachytene spermatocytes [28, 29], which was different from the results of our *in vitro* differentiation model. Our results supported the possibility that PIWIL2 might have different roles in human spermatogenesis and revealed its importance in formation and maintenance of human SSCs.

Wnt signaling pathway plays important roles in embryonic germ cells development and spermatogenesis in mice [42], also regulates the self-renewal and proliferation of mouse SSCs [43–45]. Wnt signaling pathway activates EMOES, which in turn induces human PGCLC specification by upregulating SOX17 [46]. The role of Wnt signaling pathway in formation, maintenance and differentiation of human SSCs was not clear. Using an *in vitro* differentiation model, our study proposed that Wnt signaling pathway was involved in the formation and maintenance of human SSCs, and deletion of PIWIL2 affected the expression of genes in Wnt signaling pathway, which might in turn impair the formation and maintenance of human SSCs. Wnt signaling pathway might be a target to further investigate male infertility and develop relevant therapies to reconstruct spermatogenesis.

Conclusions

In summary, our study reported the genotype-phenotype correlation of the LoF variant in *PIWIL2* and provided direct evidence that the LoF variant in *PIWIL2* impaired the formation and maintenance of human SSCs using *in vitro* differentiation model. Our results highlighted the application of *in vitro* differentiation models to functional experiments, using these models, we proposed the role of PIWIL2 in formation and maintenance of human SSCs, which was different from mouse MILI. We showed that Wnt signaling pathway was dysregulated during SSCLC induction from patient and *PIWIL2*$^{-/-}$ hiPSCs. Further research on the mechanism linking PIWIL2 and Wnt signaling is warranted. Furthermore, independent studies are needed to validate the correlation between *PIWIL2* and SCOS, before *PIWIL2* could be considered for clinical genetic tests and counseling.

Abbreviations

DEG
differentially expressed gene
FDR
false discovery rate
hiPSC
human induced pluripotent stem cell
LoF
loss-of-function
MAF
minor allele frequency
NOA
non-obstructive azoospermia
PGCLC
primordial germ cell-like cell
SCOS
Sertoli cell-only syndrome
SSCLC
spermatogonial stem cell-like cells
WES
whole exome sequencing.

Declarations

Acknowledgements

We thank the family for their support and participating in this study.

Authors' contributions

H.L., C.X., X.W. and Z.L. conceived and designed the study. H.L. and C.X. recruited the family and collected the samples. X.W., Z.L. and M.Q. performed genetic studies and functional experiments. X.W. and M.Q. performed data analysis and drafted the manuscript. H.L. and C.X. revised the manuscript. All authors read and approved the final manuscript.

Funding

This work was supported by the National Key Research and Development Program of China (No. 2017YFC1002000 to H. L.), Research Grant from Wuhan Science and Technology Bureau (No. 2018060401011317 to H. L.), Postdoctoral Science Foundation Fund of China (No. M2021M691143 to Z. L.) and PhD research startup foundation of the Third Affiliated Hospital of Zhengzhou University (to X. W.).

Availability of data and materials

The datasets supporting the conclusions of this article are included in this article.

Ethics approval and consent to participate

The study has been approved by The Ethics Committee of Tongji Medical College, Huazhong University of Science and Technology (IORG No: IORG0003571, S096).

Consent for publication

Not applicable.

Competing interests

The authors declare no competing interests.

References

1. Krausz C, Riera-Escamilla A. Genetics of male infertility. Nat Reviews Urol. 2018;15:369–84.
2. Kasak L, Laan M. Monogenic causes of non-obstructive azoospermia: challenges, established knowledge, limitations and perspectives. Hum Genet. 2021;140:135–54.
3. Fakhro KA, Elbardisi H, Arafa M, Robay A, Rodriguez-Flores JL, Al-Shakaki A, et al. Point-of-care whole-exome sequencing of idiopathic male infertility. Genet Sci. 2018;20:1365–73.
4. Abofoul-Azab M, Lunenfeld E, Levitas E, Zeadna A, Younis J, Bar-Ami S, et al. Identification of Premeiotic, Meiotic, and Postmeiotic Cells in Testicular Biopsies Without Sperm from Sertoli Cell-Only Syndrome Patients. Int J Mol Sci. 2019;20:470.
5. Yu Q, Gu X, Shang X, Li H, Xiong C. Discrimination and characterization of Sertoli cell-only syndrome in non-obstructive azoospermia using cell-free seminal DDX4. Reprod Biomed Online. 2016;33:189–96.
6. Costoya JA, Hobbs RM, Barna M, Cattoretti G, Manova K, Sukhwani M, et al. Essential role of Plzf in maintenance of spermatogonial stem cells. Nat Genet. 2004;36:653–9.
7. Yamaji M, Seki Y, Kurimoto K, Yabuta Y, Yuasa M, Shigeta M, et al. Critical function of Prdm14 for the establishment of the germ cell lineage in mice. Nat Genet. 2008;40:1016–22.
8. Weber S, Eckert D, Nettersheim D, Gillis AJM, Schäfer S, Kuckenberg P, et al. Critical function of AP-2 gamma/TCFAP2C in mouse embryonic germ cell maintenance. Biol Reprod. 2010;82:214–23.
9. Oatley MJ, Kaucher AV, Racicot KE, Oatley JM. Inhibitor of DNA Binding 4 Is Expressed Selectively by Single Spermatogonia in the Male Germline and Regulates the Self-Renewal of Spermatogonial Stem Cells in Mice1. Biol Reprod. 2011;85:347–56.
10. Wang XN, Li ZS, Ren Y, Jiang T, Wang YQ, Chen M, et al. The Wilms Tumor Gene, Wt1, Is Critical for Mouse Spermatogenesis via Regulation of Sertoli Cell Polarity and Is Associated with Non-

Obstructive Azoospermia in Humans. Hastie N, editor. PLoS Genetics. 2013;9:e1003645.

11. Kato Y, Alavattam KG, Sin H-S, Meetei AR, Pang Q, Andreassen PR, et al. FANCB is essential in the male germline and regulates H3K9 methylation on the sex chromosomes during meiosis. Hum Mol Genet. 2015;24:5234–49.
12. Kasak L, Punab M, Nagirnaja L, Grigorova M, Minajeva A, Lopes AM, et al. Bi-allelic Recessive Loss-of-Function Variants in FANCM Cause Non-obstructive Azoospermia. Am J Hum Genet. 2018;103:200–12.
13. Krausz C, Riera-Escamilla A, Chianese C, Moreno-Mendoza D, Ars E, Rajmil O, et al. From exome analysis in idiopathic azoospermia to the identification of a high-risk subgroup for occult Fanconi anemia. Genet Sci. 2019;21:189–94.
14. Yin H, Ma H, Hussain S, Zhang H, Xie X, Jiang L, et al. A homozygous FANCM frameshift pathogenic variant causes male infertility. Genet Med. 2019;21:266.
15. Araujo TF, Friedrich C, Grangeiro CHP, Martelli LR, Grzesiuk JD, Emich J, et al. Sequence analysis of 37 candidate genes for male infertility: challenges in variant assessment and validating genes. Andrologia. 2020;8:434–41.
16. Sada A, Suzuki A, Suzuki H, Saga Y. The RNA-binding protein NANOS2 is required to maintain murine spermatogonial stem cells. Science. 2009;325:1394–8.
17. Agbor VA, Tao S, Lei N, Heckert LL. A Wt1-Dmrt1 transgene restores DMRT1 to sertoli cells of Dmrt1(-/-) testes: a novel model of DMRT1-deficient germ cells. Biol Reprod. 2013;88:51.
18. Oud MS, Volozonoka L, Smits RM, Vissers LELM, Ramos L, Veltman JA. A systematic review and standardized clinical validity assessment of male infertility genes. Hum Reprod. 2019;34:932–41.
19. Fang F, Li Z, Zhao Q, Li H, Xiong C. Human induced pluripotent stem cells and male infertility: an overview of current progress and perspectives. Hum Reprod. 2018;33:188–95.
20. Sasaki K, Yokobayashi S, Nakamura T, Okamoto I, Yabuta Y, Kurimoto K, et al. Robust In Vitro Induction of Human Germ Cell Fate from Pluripotent Stem Cells. Cell Stem Cell. 2015;17:178–94.
21. Li Z, Fang F, Zhao Q, Li H, Xiong C. Supplementation of vitamin C promotes early germ cell specification from human embryonic stem cells. Stem Cell Res Ther. 2019;10:324.
22. Wang X, Qu M, Li Z, Long Y, Hong K, Li H. Valproic acid promotes the in vitro differentiation of human pluripotent stem cells into spermatogonial stem cell-like cells. Stem Cell Res Ther. 2021;12:553.
23. Zhao Y, Ye S, Liang D, Wang P, Fu J, Ma Q, et al. In Vitro Modeling of Human Germ Cell Development Using Pluripotent Stem Cells. Stem Cell Reports. 2018;10:509–23.
24. Easley CA, Phillips BT, McGuire MM, Barringer JM, Valli H, Hermann BP, et al. Direct Differentiation of Human Pluripotent Stem Cells into Haploid Spermatogenic Cells. Cell Rep. 2012;2:440–6.
25. Li Y, Wang Y, Wen Y, Zhang T, Wang X, Jiang C, et al. Whole-exome sequencing of a cohort of infertile men reveals novel causative genes in teratozoospermia that are chiefly related to sperm head defects. Hum Reprod. 2021;37:152–77.

26. Gou L-T, Kang J-Y, Dai P, Wang X, Li F, Zhao S, et al. Ubiquitination-Deficient Mutations in Human Piwi Cause Male Infertility by Impairing Histone-to-Protamine Exchange during Spermiogenesis. Cell. 2017;169:1090–104.e13.
27. Alhathal N, Maddirevula S, Coskun S, Alali H, Assoum M, Morris T, et al. A genomics approach to male infertility. Genet Med. 2020;22:1967–75.
28. Kuramochi-Miyagawa S. Mili, a mammalian member of piwi family gene, is essential for spermatogenesis. Development. 2004;131:839–49.
29. Unhavaithaya Y, Hao Y, Beyret E, Yin H, Kuramochi-Miyagawa S, Nakano T, et al. MILI, a PIWI-interacting RNA-binding Protein, Is Required for Germ Line Stem Cell Self-renewal and Appears to Positively Regulate Translation. J Biol Chem. 2009;284:6507–19.
30. Gomes Fernandes M, He N, Wang F, Van Iperen L, Eguizabal C, Matorras R, et al. Human-specific subcellular compartmentalization of P-element induced wimpy testis-like (PIWIL) granules during germ cell development and spermatogenesis. Hum Reprod. 2018;33:258–69.
31. Fang F, Li Z, Zhao Q, Xiong C, Ni K. Analysis of multi-lineage gene expression dynamics during primordial germ cell induction from human induced pluripotent stem cells. Stem Cell Res Ther. 2020;11:100.
32. Wang X, Xie S, Li Z, Ye Z, Gu X, Zhou L, et al. Generation of an iPSC line (HUSTi002-A) from fibroblasts of a patient with Sertoli cell-only syndrome carrying c.731_732delAT in PIWIL2 gene. Stem Cell Res. 2020;42:101703.
33. Bu D, Luo H, Huo P, Wang Z, Zhang S, He Z, et al. KOBAS-i: intelligent prioritization and exploratory visualization of biological functions for gene enrichment analysis. Nucleic Acids Res. 2021;49:W317–25.
34. Yan KS, Yan S, Farooq A, Han A, Zeng L, Zhou M-M. Structure and conserved RNA binding of the PAZ domain. Nature. 2003;426:468–74.
35. Sasaki T, Shiohama A, Minoshima S, Shimizu N. Identification of eight members of the Argonaute family in the human genome. Genomics. 2003;82:323–30.
36. Gu A, Ji G, Shi X, Long Y, Xia Y, Song L, et al. Genetic variants in Piwi-interacting RNA pathway genes confer susceptibility to spermatogenic failure in a Chinese population. Hum Reprod. 2010;25:2955–61.
37. Larriba S, Muñoz X, Navarro M, Mata A, Bassas L. Association of PIWIL4 genetic variants with germ cell maturation arrest in infertile Spanish men. Asian J Androl. 2014;16:931.
38. Liu X, Xi Q, Li L, Wang Q, Jiang Y, Zhang H, et al. Targeted Next-Generation Sequencing Identifies Novel Sequence Variations of Genes Associated with Nonobstructive Azoospermia in the Han Population of Northeast China. Med Sci Monit. 2019;25:5801–12.
39. Iwasaki YW, Siomi MC, Siomi H. PIWI-Interacting RNA. Its Biogenesis and Functions. Annu Rev Biochem. 2015;84:405–33.
40. Bao J, Zhang Y, Schuster AS, Ortogero N, Nilsson EE, Skinner MK, et al. Conditional inactivation of Miwi2 reveals that MIWI2 is only essential for prospermatogonial development in mice. Cell Death &

Differentiation. 2014;21:783–96.
41. Li L, Yang R, Yin C, Kee K. Studying human reproductive biology through single-cell analysis and in vitro differentiation of stem cells into germ cell-like cells. Hum Reprod Update. 2020;26:670–88.
42. Dong W-L, Tan F-Q, Yang W-X. Wnt signaling in testis development: Unnecessary or essential? Gene. 2015;565:155–65.
43. Golestaneh N, Beauchamp E, Fallen S, Kokkinaki M, Uren A, Dym M. Wnt signaling promotes proliferation and stemness regulation of spermatogonial stem/progenitor cells. Reproduction. 2009;138:151–62.
44. Takase HM, Nusse R. Paracrine Wnt/β-catenin signaling mediates proliferation of undifferentiated spermatogonia in the adult mouse testis. Proc Natl Acad Sci U S A. 2016;113:E1489–97.
45. Chassot A-A, Le Rolle M, Jourden M, Taketo MM, Ghyselinck NB, Chaboissier M-C. Constitutive WNT/CTNNB1 activation triggers spermatogonial stem cell proliferation and germ cell depletion. Dev Biol. 2017;426:17–27.
46. Mäkelä J-A, Koskenniemi JJ, Virtanen HE, Toppari J. Testis Development. Endocr Rev. 2019;40:857–905.

Tables

Table 1
Clinical parameters of the man with complete SCOS included in this study

Parameters	Refence values	Detection values
Age		42
Testis volume: left (mL)	≥ 12	5
Testis volume: right (mL)	≥ 12	5
Testis biopsy		SCOS
Karyotype		46, XY
Microdeletions of Y chromosome		Not detected
Hormone analysis		
Total testosterone (nM/L)	10.41–19.78	11.93
Free testosterone (nM/L)	0.11–0.66	0.27
FSH (IU/L)	1.27–19.26	37.72
LH (IU/L)	1.24–8.62	12.56
SHBG (nM/L)	13.2–89.5	25.7
Semen analysis		
Semen volume (mL)	≥ 1.5	5.4
Total sperm count (10^6/ejaculate)	≥ 39	0
Seminal neutral alpha-glucosidase (IU/L)	35.1–87.7	74.55
Seminal fructose (g/L)	2.95–3.35	42.24
Seminal elastase (ng/mL)	< 290	1920.5
Seminal *DDX4* mRNA		Not detected

Figures

Figure 1

Identification of a homozygous frameshift deletion variant in *PIWIL2* gene in a man with complete SCOS
(A) The patient (IV 1) came from a consanguineous family where his father (III 1) and mother were first-cousins, and his siblings were fertile. (B) Sanger sequencing confirmed the homozygous c.731_732delAT variant in *PIWIL2* in the patient and the same variant in heterozygosis in his father and brother (IV 2). (C) The homozygous c.731_732delAT variant located in exon 6 of *PIWIL2*. This variant introduced a

premature stop codon that resulted in a truncated PIWIL2 protein (273 aa), which lacked functional domains of PIWIL2 protein. (D) H&E stained testicular sections of the patient showed no spermatogenic cells existed in seminiferous tubules and only Sertoli cells arranged on the membrane in all observed seminiferous tubules. (E) Immunohistochemical detection of PIWIL2 with an antibody whose antigen was the middle part of PIWIL2 in testicular sections of the patient and man with normal spermatogenesis. No positive signal was observed in testicular tissue of the patient (Left and Right). PIWIL2 is expressed in spermatogonium, spermatocytes and spermatids in testicular tissue of man with normal spermatogenesis (Positive control).

Figure 2

Differentiation of hiPSC lines into germ cell-like cells (A) Western blot detected the expression of PIWIL2 using an antibody whose antigen was the middle part of PIWIL2 in human testis with normal spermatogenesis, human fibroblasts, and different hiPSC lines. Very faint band appeared in *PIWIL2*$^{-/-}$ hiPSCs might because the antibody bound to nonspecific proteins. (B) PGCLCs were stained with ITGA6 and EpCAM and the percentage of PGCLCs reflecting the PGCLC induction efficiency was determined at 4 days of differentiation. n = 3, n.s., not significant. (C) SSCLCs were stained with PLZF and the percentage of SSCLCs reflecting the SSCLC induction efficiency was determined at 8,10,12 and 14 days of differentiation. n = 3, * versus Control, # versus *PIWIL2*$^{+/-}$, $p < 0.05$. (D) Detection of SSC-related gens in the control, *PIWIL2*$^{-/-}$, *PIWIL2*$^{+/-}$ and patient groups by RT-qPCR at 12 days of differentiation. n = 3, * versus Control, # versus *PIWIL2*$^{+/-}$, $p < 0.05$. (E) Immunofluorescence staining of PLZF (green) and GPR125 (red) in the control, *PIWIL2*$^{-/-}$, *PIWIL2*$^{+/-}$ and patient groups at 12 days of differentiation. The nuclei were stained with DAPI (blue). PLZF^{+}/GPR125^{+} cells represented SSCLCs, they had relatively small nuclei and grew in clusters. There were less PLZF^{+}/GPR125^{+} cells in the patient and *PIWIL2*$^{-/-}$ groups, but cells with larger nuclei representing different differentiated cells.

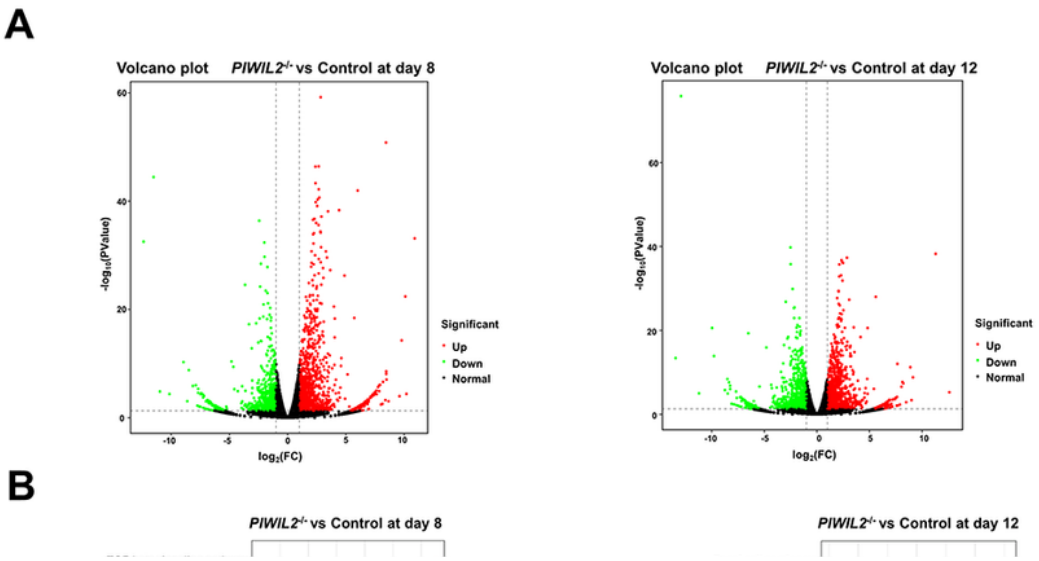

Figure 3

Transcriptome analysis of cells at 0, 8, and 12 days of SSCLC induction (A) Volcano plots of comparison of transcriptome between the control and *PIWIL2*$^{-/-}$ groups at 8 and 12 days of differentiation. Red dots represented up-regulated genes, green dots represented down-regulated genes and black dots represented genes not significantly changed. (B) KEGG analysis on the downregulated genes at 8 and 12 days of differentiation. (C) The expression of genes in Wnt signaling pathway, pluripotency, SSC, spermatocyte,

endoderm, mesoderm and ectoderm in the control and *PIWIL2*$^{-/-}$ groups at 0, 8, and 12 days of differentiation. (D) RT-qPCR confirmed the expression of genes in Wnt signaling pathway and pluripotency in the control and *PIWIL2*$^{-/-}$ groups at 8 and 12 days of differentiation. n = 3, * versus Control, # versus *PIWIL2*$^{+/-}$, $p < 0.05$.

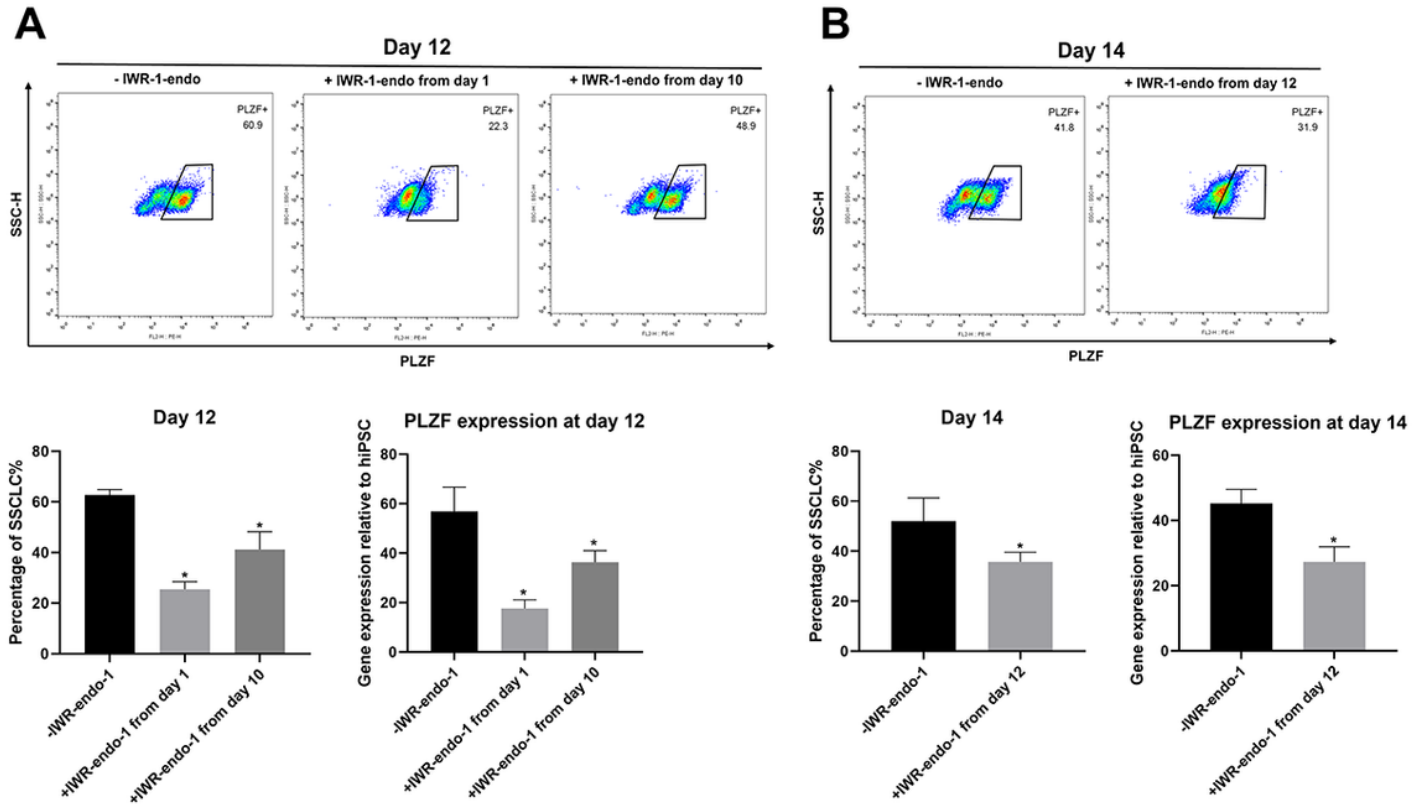

Figure 4

Inhibition of Wnt signaling pathway impaired formation and maintenance of SSCLCs (A) Wnt signaling pathway inhibitor IWR-endo-1 was added into the SSCLC induction medium from 1 day or 10 days of differentiation, and the percentage of SSCLCs was determined at 12 days of differentiation. The expression of *PLZF* was also determined by RT-qPCR at 12 days of differentiation. n = 3, * versus - IWR-endo-1, $p < 0.05$. (B) Wnt signaling pathway inhibitor IWR-endo-1 was added into the SSCLC induction medium from 12 days of differentiation, and the percentage of SSCLCs was determined at 14 days of differentiation. The expression of *PLZF* was also determined by RT-qPCR at 14 days of differentiation. n = 3, * versus - IWR-endo-1, $p < 0.05$.

Supplementary Files

This is a list of supplementary files associated with this preprint. Click to download.

- renamed2b16c.docx

- TableS4.xlsx
- renamed2307f.tif
- renamed58b2b.tif
- renamed3d93d.tif